Journal of Magnetic Resonance 196 (2009) 119–126

Contents lists available at ScienceDirect

Journal of Magnetic Resonance

journal homepage: www.elsevier.com/locate/jmr

Discerning the degenerate transitions of scalar coupled ^{1}H NMR spectra: Correlation and resolved techniques at higher quantum

G.N. Manjunatha Reddy [a], T.N. Guru Row [b], N. Suryaprakash [a,*]

[a] NMR Research Centre, Indian Institute of Science, SIF, Bangalore, Karnataka 560 012, India
[b] Solid State and Structural Chemistry Unit, Indian Institute of Science, Bangalore, Karnataka 560 012, India

ARTICLE INFO

Article history:
Received 16 August 2008
Revised 14 October 2008
Available online 31 October 2008

Keywords:
Multiple quantum
Multiple quantum *J*-resolved
Scalar couplings
Spectral analyses
Degenerate transitions
Fluorinated benzamides

ABSTRACT

The blend of spin topological filtering and the spin state selective detection of single quantum transitions by the two dimensional multiple quantum-single quantum correlation and higher quantum resolved techniques have been employed for simplifying the complexity of scalar coupled ^{1}H NMR spectra. The conventional two dimensional COSY and TOCSY experiments, though identify the coupled spin networks, fail to differentiate them due to severe overlap of transitions. Non-selective excitation of homonuclear higher quantum of protons results in filtering of spin systems irrespective of their spin topologies. The spin state selection by passive ^{19}F spins provides fewer transitions in each cross section of the single quantum dimension simplifying the analyses of the complex spectra. The degenerate single quantum transitions are further discerned by spin selective double and/or triple quantum resolved experiments that mimic simultaneous heteronuclear and selective homonuclear decoupling in the higher quantum dimension. The techniques aided the determination of precise values of spectral parameters and relative signs of the couplings.

© 2008 Elsevier Inc. All rights reserved.

1. Introduction

The development of several two dimensional NMR techniques over the decades have aided the analyses of very complex ^{1}H NMR spectra of molecules [1–3]. The identification of the group of resonances pertaining to different inequivalent protons and their coupling network is generally obtained from the conventional two dimensional COSY and TOCSY experiments [1]. This paves the way for the analyses of the first order spectra of weakly scalar coupled spin systems, where the chemical shift separation between the coupled spins is several orders of magnitude larger than the spin–spin couplings. For extracting the precise magnitudes of the scalar couplings in such weakly coupled spin systems several two dimensional experiments such as, *J*-resolved [4–6] and quantitative *J* correlation experiments [7–9] have been reported. Another methodology which has drawn considerable attention is the spin state selective detection, where the high field and low field components of both resolved and unresolved multiplets are either separated or individually detected, for the measurement of scalar couplings in biological macromolecules and also in high-resolution NMR studies in the solid state [10–34]. It is well know that the single quantum NMR spectra of weakly coupled spins are invariant to the change of relative signs of the couplings. Nevertheless both the magnitudes and signs of the couplings play a dominant role in assessing the stereochemistry and the conformation of biomolecules. There are several experimental schemes available in the literature to obtain information on the relative signs of couplings, viz. Z-COSY [35], Soft-COSY [36] and E-COSY [37]. Though tedious, the second order effects on the one dimensional spectra of double and triple resonance experiments also provide the relative signs of the couplings [38–40].

Our recent study employing the spin selective and non-selective multiple quantum single quantum correlation techniques have provided the magnitudes and relative signs of couplings [41] in addition to spectral simplification by the spin state selection of passive spins. The application of non-selective multiple quantum excitation with spin system filtering to unravel the overlap of transitions and to simplify the analyses of the scalar coupled complex ^{1}H spectra of difluorinated benzamides have been demonstrated by us recently [42]. The fluorinated benzamides are the class of compounds that have been used actively as drugs and finds potential applications as anti-inflammatory agents and antiviral agents [43] whose ^{1}H NMR spectra have been reported in the literature [44–46]. However, all the NMR spectral parameters are not available presumably due to many degenerate transitions arising from both the phenyl rings. Our quest for development of novel methodologies to analyze such complex spectra prompted us to synthesize additional molecules of the series, where the position of fluorine in one of the phenyl rings is systematically varied. The ^{1}H NMR spectra of this series of molecules are not only complex but the complexity drastically differs with the position of substitution of

* Corresponding author. Fax: +91 80 2360 1550.
E-mail address: nsp@sif.iisc.ernet.in (N. Suryaprakash).

1090-7807/$ - see front matter © 2008 Elsevier Inc. All rights reserved.
doi:10.1016/j.jmr.2008.10.018

fluorine in the phenyl ring. Most often several protons resonate over a narrow range resulting in the spectrum with many degenerate transitions. This severe overlap hinders the analysis of the spectrum and the extraction of complete spectral information is inhibited. Thus analyses of such spectra are not only challenging but demand the development of diverse experimental strategies appropriate for particular series of molecules. The present study reports the blend of higher quantum correlation experiments for spin system filtering and the novel spin selective triple quantum and double quantum *J*-resolved experiments. The experiments aided the discerning of the degenerate transitions, simplification of the complex ^{1}H NMR spectra and the determination of precise values of scalar couplings including their relative signs.

2. Experimental

Three isomers of difluorinated benzamides with the different substitution of fluorine in one of the phenyl ring, viz., 2-fluoro-*N*-(2-fluorophenyl)benzamide (**1**), 2-fluoro-*N*-(3-fluorophenyl)benzamide (**2**) and 2-fluoro-*N*-(4-fluorophenyl)benzamide (**3**) were prepared by the method described in the literature [47]. The starting materials [fluoro benzoyl chlorides (o, m, and p), fluoroanilines (o, m, and p), and dimethylaminopyridine (DMAP)] were all purchased from Sigma–Aldrich (Analytical Grade). The amines were further purified by distillation while the benzoyl chlorides were directly used without further purification. Dichloromethane used for the reaction was dried using calcium hydride and stored over molecular sieves. The fluorinated amines and the corresponding fluorinated benzoyl chlorides were taken in a round bottomed flask, in the presence of DMAP and dry dichloromethane and cooled to 0° C in an ice bath. The reaction was allowed to take place for a period of 10–12 h and the completion of the reaction was monitored using TLC. At the end of the reaction, the compound was isolated by solvent-extraction procedure using dichloromethane, dried using sodium sulfate and finally purified by column chromatography using silica by eluting with EtOAc (ethyl acetate)/hexane. The purity of the samples is reflected in their NMR spectra.

The isotropic solutions of the synthesized molecules were prepared in the solvent $CDCl_3$. All the experiments were carried out using Bruker DRX-500 NMR spectrometer. The proton 4Q-SQ correlation experiments were carried out on all the molecules using the multiple quantum pulse sequence reported earlier [41]. The delay, τ, required for creating the homonuclear anti phase magnetization during the evolution period was optimized for each molecule. Our previously reported spin selective double (SSDQ-*J*-Resolved) [41] and the present novel triple quantum (SS3Q-*J*-Resolved) *J*-resolved experiments have been carried out for extracting the remote couplings of smaller magnitudes. The pulse sequence for spin selective nQ-*J*-Resolved experiments is reported in Fig. 1. The acquisition and processing parameters for all the experiments are reported in the corresponding figure captions.

Fig. 1. The pulse sequence for the spin state selective SSnQ-*J*-resolved experiments. The sequence is identical to the nQ-SQ correlation except that the 180° pulse in the middle of t_1 period is non-selective for protons. The phase cycling is $\Phi_1 = \Phi_R = 0$. Other details are discussed in the text.

3. Results and discussion

3.1. Complexity of one dimensional NMR spectra

The one dimensional ^{1}H NMR spectra of the molecules along with their structures and the numbering of the interacting spins are reported in Fig. 2. The coupling of NH proton with the remaining spins is undetectable and thus the proton spectrum of each molecule pertains to the ten interacting spins with eight independent protons and two fluorine. The absence of symmetry element in the molecules indicates that the ^{1}H spectrum must display eight distinct proton chemical shifts. It is obvious from the Fig. 2 that all the spectra are complex with many degenerate or near degenerate transitions from two phenyl rings, in addition to many short and long range scalar couplings experienced by each proton. Furthermore, many protons are resonating over a narrow spectral range. The severity of the spectral complexity is evident from the one dimensional spectra of **2** and **3**, especially in **3** where all the multiplets from five protons resonate in a spectral width of less than 0.12 ppm depicting the significant loss of resolution and the challenging task in unraveling them. However, the situation is little favorable as the interacting spins between the two phenyl rings are separated by seven bonds and does not exhibit any couplings among them. Hence the spectrum of each molecule can be construed as an overlap of two independent five spin spectra, one from each phenyl ring. Nevertheless, for the unambiguous analyses the

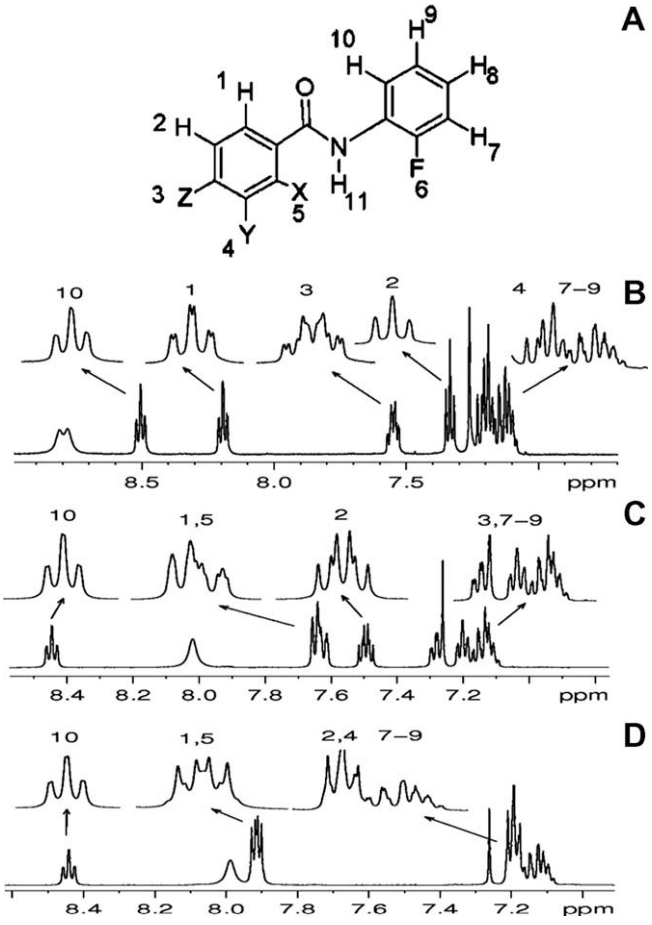

Fig. 2. (A) The structures and numbering of interacting spins in difluorinated benzamides. For molecule (**1**) X = F, Y = Z = H, for molecule (**2**) X = Z = H and Y = F and for molecule (**3**) Z = F and X = Y = H; (B–D) 500 MHz ^{1}H NMR spectra of **1**, **2** and **3**, respectively, in the solvent $CDCl_3$. The expansions of the crowded regions are depicted by arrows.

unraveling of the overlapped transitions of four protons from each phenyl ring is a dire necessity. The well known two dimensional COSY or TOCSY spectra identifies the coupled protons but fail to discriminate the spin systems of the two phenyl rings, especially those resonating in the high field region in all the molecules. This is obvious from an example of the COSY spectrum of **3** reported in Fig. 3A and in Fig. 3B, where the expanded region of 3A marked with broken rectangle is reported. Since all the spins are coupled partners, this problem remains invariant even in the TOCSY spectra (not shown). An alternate strategy would be to employ spin system filtering by manipulating their dynamics utilizing the concepts of different two dimensional NMR techniques.

3.2. Spin system filtering by employing multiple quantum coherence

Filtering of the spectrum by employing the multiple quantum coherence based on the spin topologies, viz., A_2X_2 and AX_3 etc. is reported in the literature [48,49]. As far as the spin topologies of two phenyl rings of the molecules under investigation are concerned, they are identical in **1** and are different in **2** and **3**. However, the coupled protons and fluorine of each phenyl ring in **1** and **2** pertains to the weakly coupled spin systems (as will be clear from the 4Q-SQ spectrum discussed later) of the type AFKPX, where X is the ^{19}F spin and the remaining spins are protons. It may be pointed out that in **3**; chemical structure does not imply the chemical equivalence for protons of the *para* ring. But the near/accidental equivalence provides the NMR spectrum of the type AA′MM′X. Thus the two spin systems are of the types AFKPX

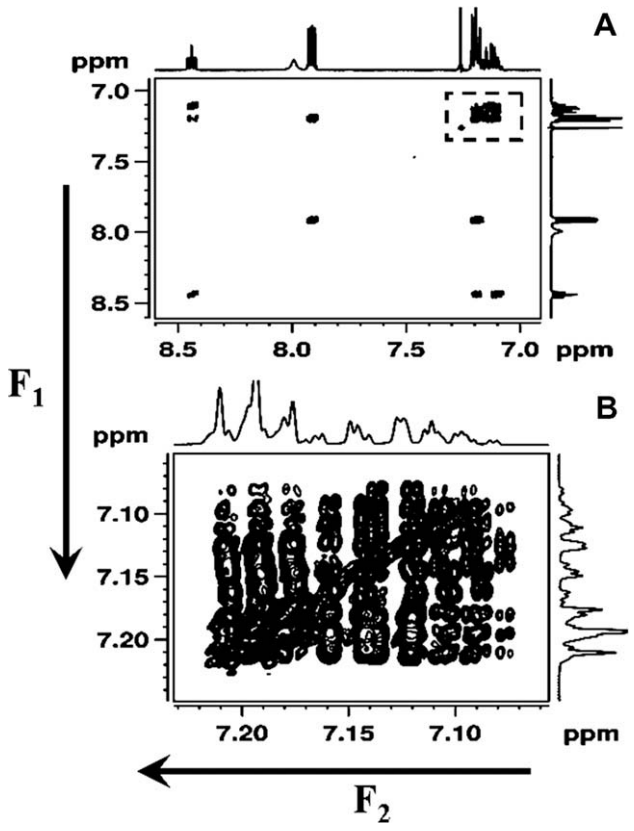

Fig. 3. (A) The homonuclear ^{1}H–^{1}H COSY spectra of **3** along with F_1 and F_2 projections. The size of the 2D data matrix is 2048 × 1024. The number of t_1 increments is 256. The time domain data was processed with the sine bell window function in both the dimensions. The digital resolution in F_1 and F_2 dimension are 0.83 and 0.41 Hz, respectively. (B) The expanded region marked with broken rectangle of Fig. 2A indicates the spectral complexity and difficulty in identifying the coupled partners.

for the phenyl rings with fluorine in the *ortho*, meta positions and AA′MM′X for ^{19}F in *para* position. ^{1}H detected spectrum is the AFKP and AA′MM′ parts of these spin systems. Nevertheless the spectrum from each phenyl ring is still complex as each proton experiences three homonuclear couplings and one heteronuclear coupling. However, in all the molecules, irrespective of the spin topologies of the phenyl rings the chemical environments of the spin systems are distinctly different. This implies that the cumulative additive values of chemical shifts of inequivalent protons of each phenyl ring are different and permits the simultaneous non-selective excitation of two homonuclear 4th quantum coherence for all the molecules. This concept is exploited for spin system filtering, i.e., for complete unraveling of the spectra of each phenyl ring.

3.3. Analysis of 4Q-SQ correlated spectra

The non-selective excitation of all the coupled protons utilizing the hard pulse leads to the spin selective excitation of 4th quantum (4Q) of the heteronuclear five spin systems. This is a situation where all the coupled protons are active spins and ^{19}F is a passive spin. With the simultaneous flipping of all the coupled protons, the five spin system of the type AFKPX or AA′MM′X behaves like an AX spin system in the 4Q dimension, where A (all the four coupled protons) is the super (active) spin and X (fluorine) is the spectator (passive) spin. The detection in the 4Q dimension is A part of this AX spin system. In the 4Q dimension the protons evolve only under the sum of passive (heteronuclear) couplings and at the cumulative additive values active chemical shifts (protons). This enables the discrimination of two independent spin systems of each molecule. However, the spin states of ^{19}F remain unperturbed in both 4Q and SQ dimensions providing the spin state selection. Thus each super spin exhibits independent doublet corresponding to spin states |α> and |β> of ^{19}F in the 4Q dimension with the separation corresponding to sum of all the heteronuclear couplings. The cross section taken parallel to the single quantum dimension at any of the ^{19}F spin states, for each phenyl ring, mimics the ^{19}F decoupling and contains transitions reduced by a factor of four, but suffice for the determination of the scalar couplings among the protons of that particular phenyl ring. Thus the analysis of the spectrum of each cross section and the extraction of the couplings is significantly simplified. In addition at each chemical shift position of ^{1}H, the cross sections are displaced along F_1 dimension corresponding to |α> and |β> spin states of ^{19}F. The magnitudes and the directions of the displacement of the cross sections provide the heteronuclear couplings and their relative signs analogous to that of an E-COSY spectrum [37]. Therefore, the experimental methodology has numerous advantages, viz., (a) filters the sub-spectra for different spin systems, (b) reduces the redundancy in the single quantum transitions for each spin state of ^{19}F, (c) simplifies the complexity of the spectrum by a factor of four, as far as the determination of the scalar couplings between the active spins is concerned and (d) provides relative signs of the heteronuclear couplings.

The ^{1}H 4Q-SQ correlated spectra of **1–3** reported in Fig. 4 distinctly differentiates the overlapped sub-spectra of the two phenyl rings. The expanded regions of the spectra of **1** and **3** are reported in Fig. 5A and B, respectively. In **1** (Fig. 4A), the difference in the cumulative additive values of all the proton chemical shifts between the phenyl rings $(\delta_{H1}+\delta_{H2}+\delta_{H3}+\delta_{H4})-(\delta_{H7}+\delta_{H8}+\delta_{H9}+\delta_{H10})_{\text{is}}$ 171.54 Hz and the corresponding value in the 4Q dimension is 171.43 Hz. In the indirect dimension, the multiplicity pattern based on the spin topology of the phenyl rings enabled the assignment of the doublet centered at 6.88 ppm to the phenyl ring with spins numbered 1–5. Accordingly the other doublet centered at 6.54 ppm is assigned to the phenyl ring with spins numbered 6–10. The respective doublet separation in the 4Q dimension for

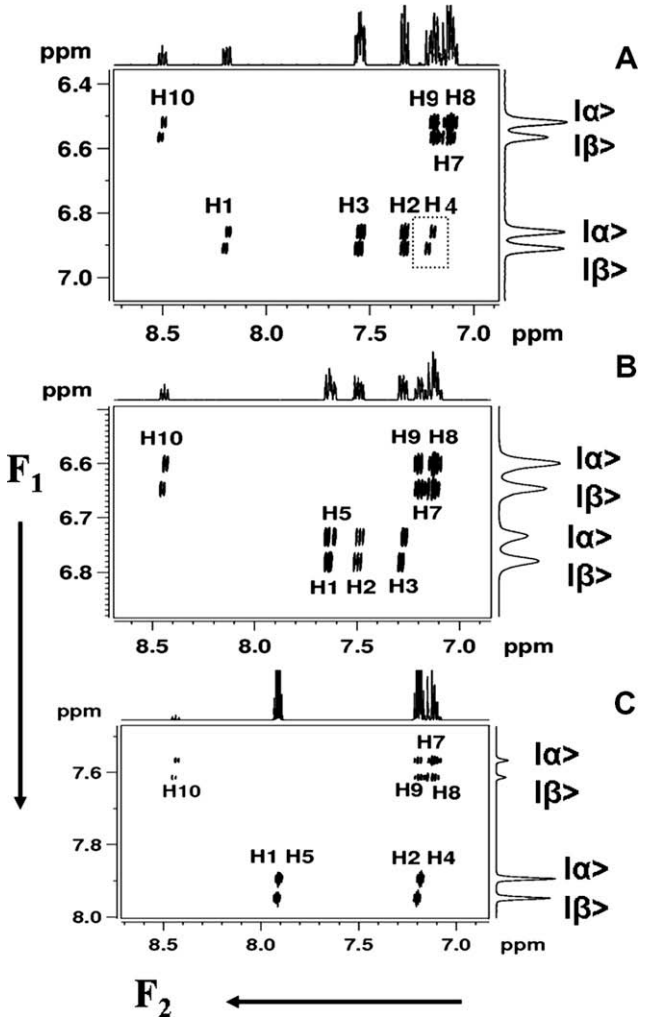

Fig. 4. (A–C) The 500 MHz ^{1}H 4Q-SQ correlated spectra of the molecules **1**, **2** and **3**, respectively, along with F_1 and F_2 projections. The assignments of chemical shifts for different protons are also marked for each molecule. The four transitions in the 4Q dimension pertain to two spin states of ^{19}F of each phenyl ring marked |α> and |β>, respectively. For A the size of the 2D data matrix is 4096 × 1024. The optimized τ delay is 35.7 ms. The digital resolution in F_1 and F_2 dimensions are 1.66 and 0.23 Hz, respectively. For B the size of the 2D data matrix is 4096 × 1024. The optimized τ delay is 166.7 ms. The digital resolution in F_1 and F_2 dimensions are 1.26 and 0.23 Hz, respectively. For C the size of the 2D data matrix is 4096 × 1024. The optimized τ delay is 35.7 ms. The digital resolution in F_1 and F_2 dimensions are 0.49 and 0.23 Hz, respectively. The time domain data of all the molecules were processed with the sine bell window function in both the dimensions.

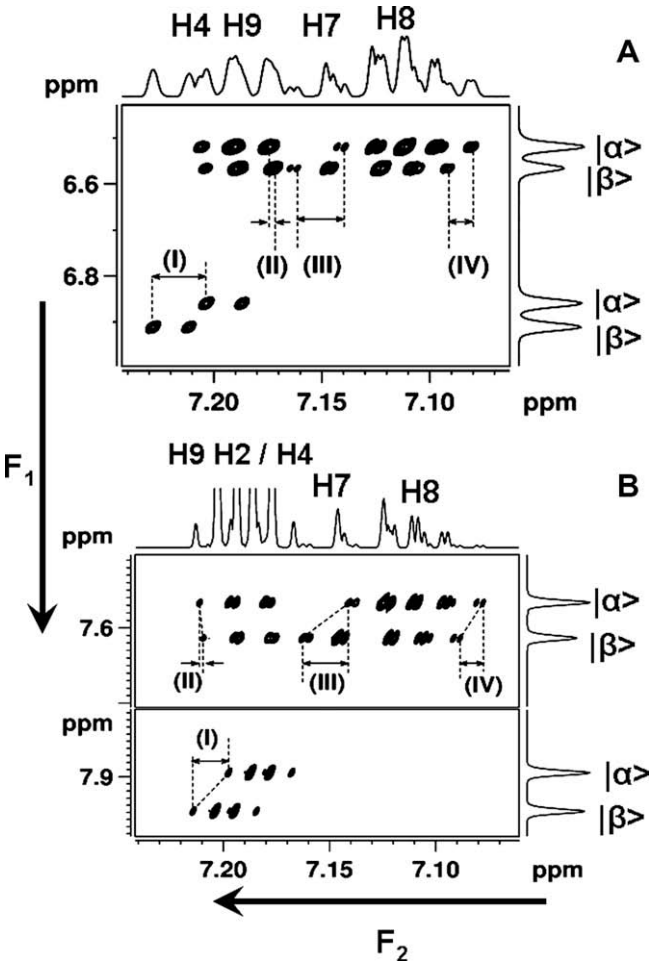

Fig. 5. (A) The expanded region of Fig. 3A for protons numbered 4 and 7–9. (B) The expanded region of Fig. 3C for protons numbered 2,4 and 7–9. The marked directions of displacements, I, II, III and IV corresponds to protons 4,9, 7 and 8 in A and 2/4, 9,7 and 8 in B, respectively. Notice the tilt of the displacement in II is opposite to that of the remaining three indicating the opposite sign of this heteronuclear coupling in both the molecules.

these rings are 23.06 and 25.23 Hz. These values are the cumulative additive values of the heteronuclear couplings of the corresponding phenyl rings. The simplification of the spectral complexity is obvious from the expanded region reported in Fig. 5A. The analyses of the multiplet pattern of cross sections taken along SQ dimension aided the assignment to independent protons (as marked in Fig. 4) and the determination of homonuclear couplings. The displacement of the cross sections pertaining to |α> and |β> states of ^{19}F and the inspection of their tilt at the respective chemical shift positions of protons, reported in Fig. 5A, provided magnitudes and relative signs of J_{HF}. It is clear that three heteronuclear couplings (J_{HF}) have their displacement vectors (I, III and IV) tilted in the same direction and the tilt of one of the displacement vector of J_{69} (II) is opposite to these three. The complete analyses reveals that in both the phenyl rings $^{5}J_{HF}$, i.e., J_{69} and J_{25} are opposite to that of all other heteronuclear couplings. The $^{3}J_{HF}$ being positive in such phenyl rings, $^{5}J_{HF}$ is determined to be negative. Furthermore the algebraic sum of all J_{HF} with appropriate sign combination is identical to the doublet separation in the 4Q dimension confirming the relative signs of J_{HF} thus determined are reported in Table 1. Similarly the expanded region of the spectrum of **3,** given in Fig. 5B also depicts the spin system differentiation, spectral simplification and negative sign of $^{5}J_{HF}$. The analyses of the 4Q-SQ correlation spectra of **2** and **3** given in Fig. 4B and C, was carried out in an identical manner and the discussion is the mere extension of the analogy. The determined scalar coupling values are also reported in Table 1.

In **3,** the spectrum of the phenyl ring with spins numbered 1–5 resembles that of an AA$^{/}$MM$^{/}$ spin system. The cross section taken along SQ dimension at either |α> or |β> spin state of ^{19}F provided a deceptively simple spectrum with only five transitions of significant intensities. The extraction of all the couplings with very few detectable weak transitions from the numerical calculation of the spectrum was not possible. On the other hand for the phenyl ring with spins numbered 6–10, many of the couplings could be determined and are reported in Table 1.

The severe overlap with too many transitions arising due to the presence of all the homonuclear couplings results in loss of resolution and the determination of the remote homonuclear couplings, $^{5}J_{HH}$ and in some cases $^{4}J_{HH}$, are challenging. As an example in Fig. 4A, a doublet is observed for the proton numbered 4 (marked

Table 1
The chemical shifts and the couplings determined for the molecules **1**, **2** and **3** in the solvent $CDCl_3$ by using 4Q-SQ correlation, SSDQ-*J*-resolved and SS3Q-*J*-resolved experiments. All Values of *J* are in Hz and δ in ppm. Errors of the parameters are of the order of digital resolution (maximum of two digital points) whose values are reported in the figure captions. Values in paranthesis are obtained by numerical iterations.

Parameter	Molecule			Parameter	Molecule		
	1	**2**	**3**		**1**	**2**	**3**
δ_1	8.19 (8.19)	7.67	7.94	J_{24}	1.4 (0.7)	5.4	5.1
δ_2	7.33 (7.33)	7.52	7.23	J_{25}	−0.04 (−0.04)	0.3	0.2
δ_3	7.55 (7.55)	7.30	—	J_{34}	8.3 (8.6)	8.3	8.9
δ_4	7.20 (7.21)	—	7.23	J_{35}	5.3 (5.0)	1.2	5.2
δ_5	—	7.65	7.94	J_{45}	12.2 (12.2)	9.3	9.7
δ_6	—	—	—	J_{67}	11.1 (10.9)	10.7	10.8
δ_7	7.15 (7.14)	7.17	7.17	J_{68}	5.5 (5.1)	5.3	5.7
δ_8	7.10 (7.10)	7.14	7.13	J_{69}	−1.1 (−1.1)	−1.0	-0.8
δ_9	7.19 (7.19)	7.23	7.22	$J_{6,10}$	7.8 (7.5)	8.1	8.1
δ_{10}	8.50 (8.50)	8.07	8.47	J_{78}	8.0 (8.3)	8.1	6.7
J_{12}	8.0 (8.0)	8.0	9.7	J_{79}	1.6 (1.4)	1.5	1.1
J_{13}	1.5 (1.8)	1.00	5.2	$J_{7,10}$	0.4 (0.7)	0.3	0.4
J_{14}	0.6 (0.2)	−0.2	0.2	J_{89}	6.8 (6.9)	7.1	7.1
J_{15}	8.2 (7.9)	1.2	5.1	$J_{8,10}$	1.7 (1.6)	1.8	1.7
J_{23}	7.3 (7.1)	8.6	8.3	$J_{9,10}$	9.4 (8.7)	8.2	8.2

J_{15} and J_{24} in **3** are not precise due to deceptive simplicity of the spectra.

with broken rectangle). However, the topology of the spin system suggests that $^4J_{24}$ and $^5J_{14}$ should provide additional splittings. Thus 4Q-SQ correlation experiment fails to resolve very small remote ^1H–^1H couplings. Thus the extraction of remote couplings $^5J_{14}$ and $^5J_{7,10}$ in **1** and **3** and $^5J_{25}$ and $^5J_{7,10}$ in **2** from the 4Q-SQ correlation experiments are severely hindered. These problems have been circumvented by further reducing the spectral complexity in each cross section by employing spin selected DQ and 3Q-*J*-resolved spectra discussed in the subsequent sections.

3.4. Spin selective double quantum J-resolved (SSDQ-J-resolved) experiment

One of the ways of combating the problem of determining very small couplings is achieved by homonuclear spin state selection of remote passive couplings such as $^5J_{25}$. For this to be achieved the remote proton must be a passive spin and its spin states should not be disturbed in MQ and SQ dimensions. Moreover to avoid any further displacement due to spin state selection of ^{19}F spin, the decoupling of ^{19}F spin is essential. The design of such a pulse sequence is possible by selective (in **2** and **3**) or biselective (in **1**) excitations of two spins leading to double quantum coherence. The application of a non-selective refocusing pulse in such a sequence in the middle of the t_1 dimension on protons mimics ^{19}F decoupling. This is analogous to the spin selective *J*-resolved experiment employing double quantum (DQ) excitation. This sequence developed by us recently [41] has been applied which retains both active and passive couplings in the direct dimension, decouples ^{19}F and retains only the active couplings in the double quantum dimension thereby achieving spin state selection. Though small, these remote passive couplings lead to relative displacements which are measurable in such resolved experiments.

The typical SSDQ-*J*-resolved spectra of **1** and **2** are reported in Fig. 6A and B, respectively. In **1**, as is apparent from Fig. 4A, that the phenyl ring with spins numbered 1–5 has the chemical shifts of protons well dispersed. Nevertheless the double quantum excitation of spins 2 and 4 is impossible without disturbing the spins from the other ring. However, the biselective excitation of any two spins which do not disturb the spins of the other phenyl ring is feasible. Thus the double quantum excitation of spins 1 and 3 was carried out. This retains only the sum of passive couplings to protons 2 and 4 (i.e., $J_{12}+J_{14}+J_{23}+J_{34}$) while the couplings to fluorine spin is completely refocused by a non-selective hard pulse in the middle of t_1 dimension. In such a situation the remaining two passive protons (2 and 4) of the corresponding phenyl ring mimics the heteronuclei and their spin states are not disturbed. In the spin product basis these protons have four Eigen states $|\alpha_2\alpha_4>$, $|\alpha_2\beta_4>$, $|\beta_2\alpha_4>$ and $|\beta_2\beta_4>$, where the subscript refers to protons 2 and 4. Thus the DQ dimension will have four transitions with the large doublet separation providing $J_{12}+J_{23}$, while the smaller doublet separation provides $J_{14}+J_{34}$. The separation in the DQ dimension would be identical at the chemical shift positions of both the active spins. In the SQ dimension there are two displacement vectors for each of the spins 1 and 3 which provide both active and passive couplings. The two displacements at the chemical shift position of proton 1 provide individual values of J_{12} and J_{14} as marked in Fig. 6A. The displacements at the chemical shift position of proton 3 can be exploited to derive individual values of J_{23} and J_{34}. Thus the experiment aided the precise determination of such long range couplings, which were difficult to extract from the 4Q-SQ experiment. Similar double quantum experiment with selective excitation of spins 1 and 2 also provides identical but redundant information. Similarly in the molecule **2** SSDQ-*J*-resolved spectra reported in Fig. 6B provided the remote couplings which are marked. However, for the molecule **3**, the protons of the *para* ring being strongly coupled, this SSDQ-*J*-resolved experiment is not possible. As far as the phenyl ring with spins number 6–10 is concerned, the degeneracy of transitions does not permit such double quantum excitation. This problem has been circumvented by resorting to the novel spin selective triple quantum *J*-resolved experiment.

3.5. Spin selective triple quantum J-resolved (SS3Q-J-resolved) experiment

Extraction of the coupling among protons in the phenyl ring with protons 7–10 is tedious due to severe overlap of the transitions from the protons 7, 8 and 9. This is due to identical spin topology in all the molecules. Therefore, the selective excitation of any two protons of this ring is impossible without disturbing the remaining protons. However, selective excitation of protons 7, 8 and 9 is not precluded. Analogous to SSDQ-*J*-resolved experiment, the novel SS3Q-*J*-resolved experiment has been carried out. The pulse sequence is identical to that of double quantum experiment, except that the triple quantum coherence is selected by appropriate gradient ratio. As an example the SS3Q-*J*-resolved spectra of **1** and **3**, are reported in Fig. 7A and B, respectively. The decoupling of ^{19}F by the π pulse in the t_1 dimension, provides

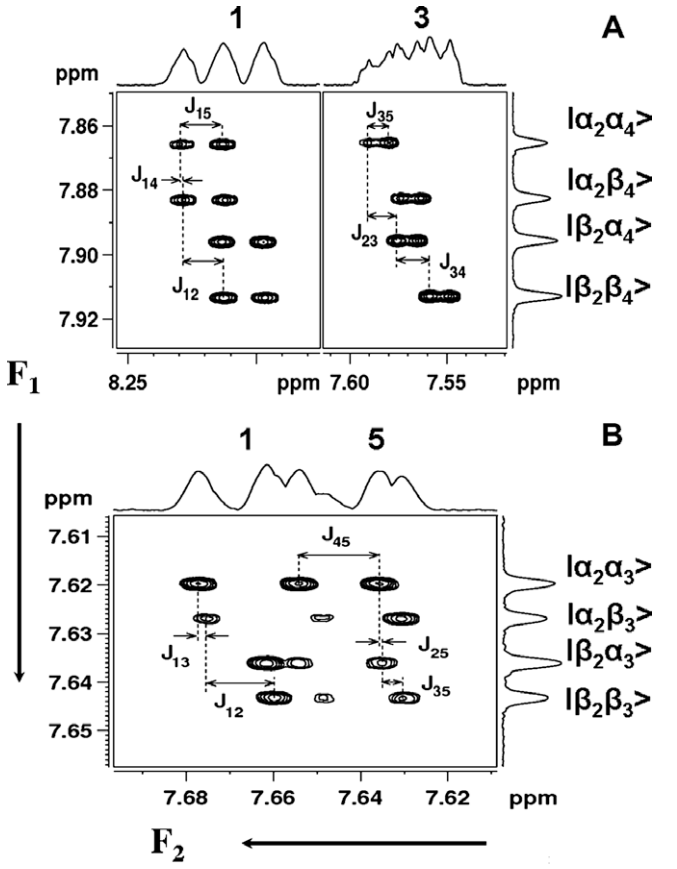

Fig. 6. (A) The SSDQ-*J*-resolved spectra of **1** in the isotropic solvent $CDCl_3$ with the biselective excitation of protons 1 and 3. The seduced shape pulses of duration 17.86 ms have been used for selective excitation. The size of the 2D data matrix is 2048 × 1024. The number of t_1 increments is 96. The time domain data was processed with the sine bell window function in both the dimensions. The digital resolution in F_1 and F_2 dimension are 0.27 and 0.04 Hz, respectively. The optimized τ delay is 125 ms. The marked spin states in the DQ dimension corresponds to the passive spins 2 and 4. The displacements providing the coupling information are; a = J_{15} b = J_{14}, c = J_{12}, d = J_{35}, e = J_{13}, f = J_{23} and g = J_{34}. Notice the smaller values of the couplings (J_{13} and J_{14}) that could be measured from this experiment which were hindered in the 4Q-SQ correlation experiment. (B) The SSDQ-*J*-resolved spectra of *ortho*, *meta*-difluorinated benzanilide in the isotropic solvent $CDCl_3$ with the selective excitation of protons 1 and 5. The marked spin states in the DQ dimension corresponds to the passive spins 2 and 3. The displacements providing the coupling information are; a′ = J_{13} b′ = J_{12}, c′ = J_{45}, d′ = J_{25}, e′ = J_{25}. Notice the smaller values of the couplings (J_{13} and J_{25}) that could be measured from this experiment which were hindered in the 4Q-SQ correlation experiment.

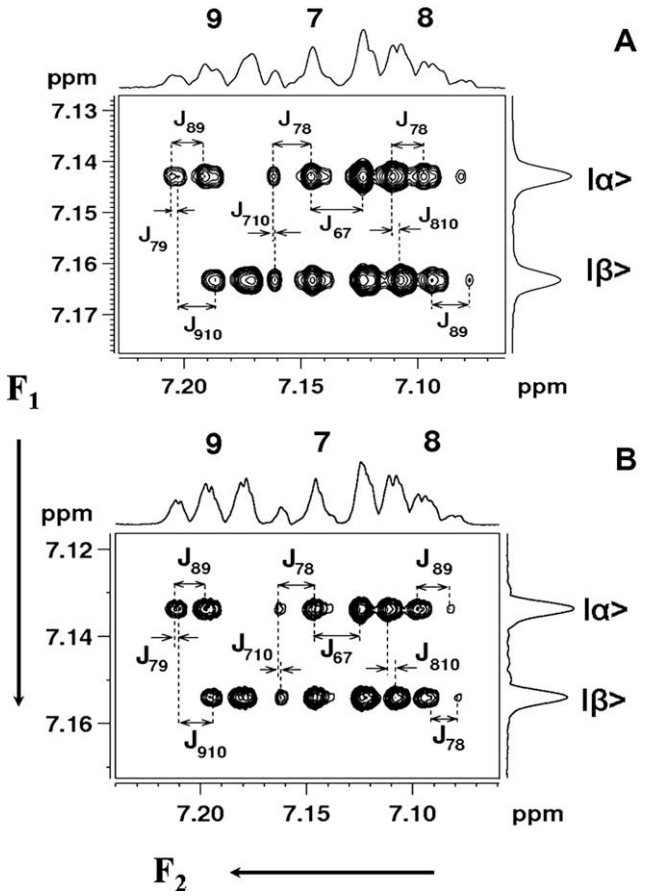

Fig. 7. (A and B) The SS3Q-*J*-resolved spectra of **1** and **3**, respectively, in the isotropic solvent $CDCl_3$ with the selective excitation of protons 7, 8 and 9. The size of the 2D data matrix is 4096 × 2048. The number of t_1 increments is 128. The time domain data was processed with the sine bell window function in both the dimensions. The digital resolution in F_1 and F_2 dimension are 0.02 and 0.01 Hz, respectively. The optimized τ delay is of duration 62.5 ms. The seduced shape pulses are of duration 8.33 and 5 ms for molecules **1** and **3**, respectively. The marked spin states |α> and |β> in the 3Q dimension corresponds to the passive spin states of proton 10. For **1**, the displacements providing the coupling information are a = J_{89}, b = J_{79}, c = J_{910}, d = J_{78}, e = $J_{7,10}$, f = J_{67}, g = J_{78}, h = $J_{8,10}$ and i = J_{89}. The corresponding values for **3** are denoted with double primes. Notice the smaller values of the coupling, $J_{7,10}$ that could be measured from this experiment which was difficult to obtain from the other experiments. The direction of the tilts indicate that the couplings $J_{7,10}$, $J_{8,10}$ and $J_{9,10}$ have similar signs.

a doublet in the 3Q dimension due to splitting from the |α> and |β> spin states of passive proton 10 with a separation equal to the sum of all the couplings to the passive spin ($J_{7,10} + J_{8,10} + J_{9,10}$). The displacement of cross sections aided the direct measure of $^3J_{HH}$, $^4J_{HH}$ and $^5J_{HH}$ to proton 10. The displacements and the resonance separations providing the couplings are marked in the figure. The inspection of the directions of the tilts marked in the figures reveals that $^3J_{HH}$, $^4J_{HH}$ and $^5J_{HH}$ with proton 10 are having similar signs. The combined analyses of 4Q-SQ correlated, SSDQ-*J*-resolved and SS3Q-*J*-resolved experiments provided the precise values of J_{HH} and J_{HF} reported in Table 1. Similar analyses of SS3Q-*J*-resolved spectra for **2** have also been carried. The precise values of long range couplings $^5J_{14}$ in **1**, $^5J_{25}$ in **2** and $^5J_{710}$ in **1**–**3** could be determined.

Both double and triple quantum *J*-resolved techniques have several distinct advantages, viz., (a) separates very small proton couplings in different dimensions, (b) reduces spectral complexity by spin state selection, (c) simultaneously decouples the fluorine to all the protons in DQ/3Q dimension, (d) displacement vector provides relative signs of the homonuclear couplings and (e) overcomes the problem of field inhomogeneity contributions due to π pulse in the middle of the t_1 dimension.

3.6. Numerical analyses of the spectra

For estimating the precision of the determinacy of the parameters obtained experimentally, the iterative analysis has also been carried out for one of the molecules in the present study. The numerical iterative analyses of one dimensional spectra are generally carried out using the initial guessed spectral parameters. The specific experimental transitions are assigned to theoretical ones and the parameters are subsequently refined by iterative calculations until the root mean square error between the theoretical and experimental transitions approach global minimum. This procedure inhibited for the molecules under investigation due to severe degeneracy of the transitions. However, the analysis of any one of the cross sections corresponding to |α> and |β> spin states of ^{19}F provides homonuclear couplings and the combined analysis

of transitions corresponding to both the spin states provides both homo and heteronuclear couplings pertaining to each phenyl ring in each molecule. To judge the efficiency of the technique employed, the computer program LEQUOR [50] was employed and the numerical iterative analyses were carried for the molecule **1** treating it as two independent five spin systems. The chemical shifts and the couplings determined by the higher quantum correlation and resolved experiments were used as the starting parameters and were iterated further. The determined parameters have also been reported in the Table 1. It is clear from the table that the experimentally measured values of couplings are in close agreement with the numerically calculated ones within the acceptable errors (digital resolution).

4. Conclusions

The analyses of one dimensional proton NMR spectra of isomers of difluorinated benzanilides are very complex and challenging. The present study exploits the difference between the cumulative additive values of proton chemical shifts of each phenyl ring for their differentiation irrespective of their spin topologies employing homonuclear fourth quantum coherence. This spin system filtering combined with spin state selective detection of single quantum transitions significantly simplifies the determination of homonuclear couplings from the ^{1}H spectra taken along the cross section of the single quantum dimension at the spin state of ^{19}F. The displacement and the direction of the tilt of the displacement vectors at the chemical shift positions of each proton provided magnitudes and relative signs of heteronuclear couplings. The spin selective double and triple quantum *J*-resolved experiments aided the determination of remote couplings of smaller magnitudes. The systematic studies reveal that in the phenyl ring systems $^{5}J_{HF}$ is negative in all the molecules irrespective of their spin topologies.

Acknowledgment

N.S. gratefully acknowledges the Department of Science and Technology, New Delhi for the financial Grant No. SR/S1/PC-13/2004.

References

[1] R.R. Ernst, G. Bodenhausen, A. Wokaun, Principles of Nuclear Magnetic Resonance in One and Two dimensions, Clarendon Press, Oxford, 1991.
[2] J. Keeler, Understanding NMR Spectroscopy, John Wiley and Sons, England, 2005.
[3] J. Cavanagh, W.J. Fairbrother, A.G. Palmer III, M. Rance, N.J. Skelton, Protein NMR Spectroscopy, second ed., Principles and Practice, Academic Press, New York, 2007.
[4] D. Neuhaus, G. Wagner, M. Vašák, J.H.R. Käegi, K. Wüthrich, Systematic application of high-resolution, phase-sensitive two-dimensional ^{1}H NMR techniques for the identification of the amino-acid-proton spin systems in proteins. Rabbit metallothionein-2, Eur. J. Biochem. 151 (1985) 257–273.
[5] L.E. Kay, A. Bax, New methods for the measurement of NH–CαH coupling constants in 15N-labeled proteins, J. Magn. Reson. 86 (1990) 10–126.
[6] S. Heikkinen, H. Aitio, P. Permi, R. Folmer, K. Lappalainen, I. Kilpeläinen, J-multiplied HSQC (MJ-HSQC): a new method for measuring 3J(HNHα) couplings in 15N-labeled proteins, J. Magn. Reson. 137 (1999) 243–246.
[7] A. Bax, D. Max, D. Zax, Measurement of long-range 13C–13C J couplings in a 20-kDa protein–peptide complex, J. Am. Chem. Soc. 114 (1992) 6923–6925.
[8] B. Reif, M. Köck, R. Kerssebaum, J. Schleucher, C. Griesinger, 1*J*, 2*J*, and 3*J* Carbon–Carbon Coupling Constants at Natural Abundance, J. Magn. Reson. B 112 (1996) 295–302.
[9] J.S. Hu, A. Bax, Determination of ϕ and χ1 angles in proteins from 13C–13C three-bond *J* couplings measured by three-dimensional heteronuclear NMR. How planar is the peptide bond?, J Am. Chem. Soc. 119 (1997) 6360–6368.
[10] W.S. Brey, L.W. Jaques, H.J. Jakobsen, A 13C-{1H} double resonance study of the signs of 1H-19F and 13C-19F spin coupling constants in fluorobenzenes and 2-fluoropyridine, Org. Magn. Reson. 12 (1979) 243–246.
[11] J. Jarvet, P. Allard, Phase-sensitive two-dimensional heteronuclear zero- and double-quantum-coherence spectroscopy, J. Magn. Reson. B 112 (1996) 240–244.
[12] P. Permi, S. Heikkinen, I. Kilpeläinen, A. Annila, Measurement of homonuclear 2*J*-couplings from spin-state selective double-/zero-quantum two-dimensional NMR spectra, J. Magn. Reson. 139 (1999) 273–280.
[13] G. Otting, A DQ/ZQ NMR experiment for the determination of the signs of small *J*(1H,13C) coupling constants in linear spin systems, J. Magn. Reson. 124 (1997) 503–505.
[14] A. Rexroth, P. Schmidt, S. Szalma, T. Geppert, H. Schwalbe, C. Griesinger, New principle for the determination of coupling constants that largely suppresses differential relaxation effects, J. Am. Chem. Soc. 117 (1995) 10389–10390.
[15] P. Anderson, J. Weigelt, G. Otting, Spin-state selection filters for the measurement of heteronuclear one-bond coupling constants, J. Biomol. NMR 12 (1998) 435–441.
[16] B. Brutscher, Accurate measurement of small Spin–Spin couplings in partially aligned molecules using a novel *J* -mismatch compensated spin-state-selection filter, J. Magn. Reson. 151 (2001) 332–338.
[17] P. Permi, Determination of three-bond scalar coupling between 13C′ and 1Hα in proteins using an iHN(CA),CO(α/β-*J*-COHA) experiment, J. Magn. Reson. 163 (2003) 114–120.
[18] L. Duma, S. Hediger, A. Lesage, L. Emsley, Spin-state selection in solid-state NMR, J. Magn. Reson. 164 (2003) 187–195.
[19] L. Duma, S. Hediger, B. Brutscher, A. Böckmann, L. Emsley, Resolution enhancement in multidimensional solid-state NMR spectroscopy of proteins using spin-state selection, J. Am. Chem. Soc. 125 (2003) 11816–11817.
[20] P. Nolis, J.F. Espinosa, T. Parella, Optimum spin-state selection for all multiplicities in the acquisition dimension of the HSQC experiment, J. Magn. Reson. 180 (2006) 39–50.
[21] R. Verel, T. Manolikas, A.B. Siemer, B.H. Meier, Improved resolution in 13C solid-state spectra through spin-state-selection, J. Magn. Reson. 184 (2007) 322–329.
[22] P. Permi, A. Annila, A new approach for obtaining sequential assignment of large proteins, J. Biomol. NMR 20 (2001) 127–133.
[23] P. Permi, A. Annila, Transverse relaxation optimised spin-state selective NMR experiments for measurement of residual dipolar couplings, J. Biomol. NMR 16 (2000) 221–227.
[24] P. Permi, A spin-state-selective experiment for measuring heteronuclear one-bond and homonuclear two-bond couplings from an HSQC-type spectrum, J. Biomol. NMR 22 (2002) 27–35.
[25] D. Lee, B. Vögeli, K. Pervushin, Detection of C′, Cα correlations in proteins using a new time- and sensitivity-optimal experiment, J. Biomol. NMR 31 (2005) 273–278.
[26] P. Würtz, K. Fredriksson, P. Permi, A set of HA-detected experiments for measuring scalar and residual dipolar couplings, J. Biomol. NMR 31 (2005) 321–330.
[27] C.R.R. Grace, R. Riek, Pseudomultidimensional NMR by spin-state selective off-resonance decoupling, J. Am. Chem. Soc. 125 (2003) 16104–16113.
[28] P. Nolis, T. Parella, Simultaneous α/β spin-state selection for 13C and 15N from a time-shared HSQC-IPAP experiment, J. Biomol. NMR 37 (2007) 65–77.
[29] P.R. Vasos, J.B. Hall, D. Fushman, Spin-state selection for increased confidence in cross-correlation rates measurements, J. Biomol. NMR 31 (2005) 149–154.
[30] L. Braunschweiler, G. Bodenhausen, R.R. Ernst, Analysis of networks of coupled spins by multiple quantum NMR, Mol. Phys. 48 (1983) 535–560.
[31] G K Pierens, T A Carpenter, L.D. Colebrook, L.D. Field, L.D. Hall, Selection of multiple-quantum spectra of molecules in liquid-crystalline solution using pulsed magnetic field gradients, J. Magn. Reson. 99 (1992) 398–402.
[32] J.M. Polson, E.E. Burnell, A multiple-quantum 1H NMR study of partially oriented biphenylene, J. Magn. Reson. A 106 (1994) 223–228.
[33] J.C.T. Rendell, E.E. Burnell, Frequency-selective excitation in multiple-quantum NMR, J. Magn. Reson. A 112 (1995) 1–6.
[34] T. Chandrakumar, J.M. Polson, E.E. Burnell, A multiple-quantum ^{1}H NMR study of conformational biasing of biphenyl in a nematic liquid crystal, J. Magn. Reson. A 118 (1996) 264–271.
[35] H. Oschkinat, A. Pastore, P. Pfändler, G. Bodenhausen, Two-dimensional correlation of directly and remotely connected transitions by *z*-filtered COSY, J. Magn. Reson. 69 (1986) 559–566.
[36] R. Brüschweiler, J.C. Madsen, C. Griesinger, O.W. Sørensen, R.R. Ernst, Two-dimensional NMR spectroscopy with soft pulses, J. Magn. Reson. 73 380 (1987).
[37] C. Griesinger, O.W. Sørensen, R.R. Ernst, Two-dimensional correlation of connected NMR transitions, J. Am. Chem. Soc. 107 (1985) 6394–6396.
[38] W. McFarlane, D.S. Rycroft, Magnetic Multiple Resonance, Ann. Rep. NMR Spectr. 9 (1979) 319–414.
[39] S. Sorensen, R.S. Hansen, H.J. Jakobsen, Assignments and relative signs of 13C-X coupling constants in 13C FT NMR from selective population transfer (SPT), J. Magn. Reson. 14 (1974) 243–245.
[40] H.J. Jakobsen, T. Bundgaard, R.S. Hansen, Assignments and signs of 13C-31P coupling constants from off-resonance proton decoupled 13C spectra, Mol. Phys. 23 (1972) 197–201.
[41] B. Bikash, N. Suryaprakash, Spin selective multiple quantum NMR for spectral simplification, determination of relative signs and magnitudes of scalar couplings by spin state selection, J. Chem. Phys. 127 (2007) 214510.
[42] B. Bikash, G.N. Manjunatha Reddy, R.P. Uday, T.N. Guru Row, N. Suryaprakash, Simplifying the complex ^{1}H NMR spectra of fluorine substituted benzamides by spin system filtering and spin state selection: multiple quantum-single quantum correlation, J. Phys. Chem. A 112 (2008) 10526–10532.
[43] D. Chopra, Ph.D. Thesis, Indian Institute of Science, Bangalore, India, 2008.

[44] Y.Y. Zhu, H.P. Yi, C. Li, X.K. Jiang, Z.T. Li, Cryst. The N?H···X (X = Cl, Br, and I) hydrogen-bonding pattern in aromatic amides: a crystallographic and 1H NMR study, Crystal Growth Des. 8 (2008) 1294–1300.
[45] C. Li, S.F. Ren, J.L. Hou, H.P. Yi, S.Z. Zhu, X.K. Jiang, Z.T. Li, F···H-N Hydrogen bonding driven foldamers: efficient receptors for dialkylammonium ions, Angew Chem. Int. Ed. 44 (2005) 5725–5729.
[46] K. Waisser, J. Kuneš, J. Kubicová, M. Buděšínský, O. Exner, Polynuclear magnetic resonance of substituted thiobenzanilides and benzanilides: transmission of substituent effects through thiocarboxamide group, Magn. Reson. Chem. 35 (1997) 543–548.
[47] D. Chopra, T.N. Guru Row, Evaluation of the interchangeability of C–H and C–F groups: insights from crystal packing in a series of isomeric fluorinated benzanilides, Cryst. Eng. Comm. 10 (2008) 54–67.
[48] M.H. Levitt, R.R. Ernst, Spin-pattern recognition in high-resolution proton NMR spectroscopy, Chem. Phys. Lett. 100 (1983) 119–123.
[49] M.H. Levitt, R.R. Ernst, Multiple-quantum excitation and spin topology filtration in high-resolution NMR, J. Chem. Phys. 83 (1985) 3297–3310.
[50] P. Diehl, H.P. Kellerhals, W. Niederberger, The structure of toluene as determined by NMR of oriented molecules, J. Magn. Reson. 4 (1971) 352–357.